Translated Article

English Translation of *J. Surf. Anal.* 24, 192-205(2018), Auger Depth Profiling Analysis of HfO_2/Si Specimen Using an Ultra Low Angle Incidence Ion Beam

T. Ogiwara,[a,*] T. Nagata,[b] and H. Yoshikawa[c]

[a] *Materials Analysis Station, Research Network and Facility Services Division, National Institute for Materials Science, 1-2-1 Sengen, Tsukuba, Ibaraki 305-0047, Japan*

[b] *International Center for Materials Nanoarchitectonics, National Institute for Materials Science, 1-1 Namiki, Tsukuba, Ibaraki 305-0044, Japan*

[c] *Surface Chemical Analysis Group, Research Center for Advanced Measurement and Characterization, National Institute for Materials Science, 1-2-1 Sengen, Tsukuba, Ibaraki 305-0047, Japan*

[*] *OGIWARA.Toshiya@nims.go.jp*

(Received: March 31, 2018)

We have investigated the Auger depth profiling analysis of HfO_2/Si by the glancing-angle ion beam sputtering method at an incident angle of 7 degree from the sample surface with argon ion beam. The depth resolutions of the O KLL interface profiles were 0.9 nm and 1.5 nm, at the ion-beam acceleration voltage of 2.0 kV and 3.0 kV respectively, which were better than the depth resolutions at a commonly-used incident angle of 51 degree. However, the ion-beam-induced reduction of HfO_2 was not suppressed by the glancing-angle ion beam sputtering at the ion acceleration voltage of 0.5 kV, which is expected to be the lowest damage sputtering condition in this study. The reduction of HfO_2 due to preferential sputtering of oxygen was observed by the intensity ratio of O KLL and Hf NVV depth profiles. It was found that the ratio of preferential sputtering depends on the ion incidence angle and the ion acceleration voltage. Under the glancing-angle condition, the ratio of preferential sputtering greatly depended on the ion accelerating voltage, and it was found that the lower the ion acceleration voltage is, the easier it is for O to be sputtered than Hf. On the other hand, under the commonly-used incident angle conditions, the ratio of preferential sputtering did not depend much on the ion acceleration voltage. The dependency of the ratio of preferential sputtering on the ion incidence angle can be explained by the difference in sputtering models depending on the ion incidence angle. It was found that the O KLL depth profiles showed partial recovery of the oxygen intensity near the interface of HfO_2/Si, which can be related to oxygen generated by the ion-beam-induced decomposition of the diffusion layer at the interface. In addition, the glancing-angle ion beam enables the reduction of the effect of recoil implantation of Hf atoms into the Si substrate.

1. Introduction

Auger depth profiling with an ultra-low-angle-incidence ion beam is a sputtering method in which both electrons and ions are irradiated with incident angles of a few degrees to a sample surface by using a high-angle inclined specimen holder [1]. With the method, the ultra-low-angle-incidence electrons increase the Auger signal intensities and reduce the background, while the ultra-low-angle-incidence ions suppress the atomic mixing and greatly improve depth resolution. GaAs/AlAs multilayers [2], SiO_2/Si multilayers [3], and Si/Ge multiple delta-layer specimens [4], which are standard samples for depth profiling, have been analyzed with high sensitivities and depth resolutions in comparison with conventional methods.

Here, depth analysis of an HfO_2/Si substrate was performed to investigate the applicability of this method to practical materials. HfO_2 is a high-k, multifunctional, dielectric material [5], which are recently used for resistance-change nonvolatile memories utilizing oxygen

deficiency and ion diffusion in HfO_2 [6], and controlled ferroelectric crystals with strain in HfO_2 [7]. The compositions of the interface and the film are closely related to these functions. In the present study, we investigated the composition in the depth direction of the HfO_2/Si interface under various conditions of acceleration voltages and incidence angles of the ions with both a high-angle-inclined specimen holder and a commonly used flat holder.

The incident angle expressed in this study was defined as the angle to the sample surface, because the "low-angle incidence" of this method means the low angle to the surface, although it is usually defined by ISO 18115-1[8] as the angle to the sample normal.

2. Experimental

2.1 Angle adjustment for ultra-low-angle-incident beam Auger depth profiling

Fig.1 is an overview of the 85° high-angle-inclined specimen holder. Fig.1 (a) was the photograph taken from the front, with the sample in the holder. Fig.1 (b) was the photograph after a 90 degree-clockwise rotation. Fig.2 showed the sample holder set on the sample stage of the Auger electron spectrometer. The sample surface faced the concentric hemispherical analyzer (CHA) electron spectrometer in Fig.2 (a), while, in Fig.2 (b), the sample stage was rotated counterclockwise by 35°.When the high-angle holder was used, the electron beam was always irradiated at 5°to the sample surface, and, when the sample surface faced the spectrometer, the ion incidence angle was 35°to the sample surface. As the high-angle holder was rotated counterclockwise on the sample stage, the incident ion angle became lower. At the position in Fig.2 (b), the incident ion angle was 7°to the sample surface. In short, after the sample holder was rotated 35°counterclockwise from the position where it faced to the spectrometer, the angle of the electron beam and the ion beam were 5, and 7 degree, respectively, allowing ultra-low-angle-incident beam Auger depth profiling.

2.2 Sample

A 55 nm HfO_2 film grown on a Si (100) substrate by pulsed laser deposition [9] was used as a sample. The film was prepared as follows. The Si (100) substrate with a native oxide film was cleaned with ethanol, acetone, pure water, and UV-ozone. It was then placed in a vacuum chamber where the HfO_2 layer was deposited via ablation of a HfO_2 sintered target with KrF excimer laser pulses (248 nm wavelength). The substrate temperature was at room temperature, the oxygen partial pressure was 10^{-3} torr, and the laser repetition frequency was 5 Hz. HfO_2 films of 3 nm and 6 nm thicknesses were fabricated on the Si substrate using a shadow mask. The interface was examined by transmission electron microscopy (TEM, JEOL JEM-2100F) and X-ray photoelectron spectroscopy (XPS, Thermo Theta-probe). The accelerating voltage of TEM was 200 kV. The X-ray sources of the XPS was Al-K_α (1486.6 eV) monochromatic X-rays and the surface charging was prevented by a neutralizing gun. Angle-resolved XPS spectra of Si 2p were acquired by changing the photoelectron take-off angles.

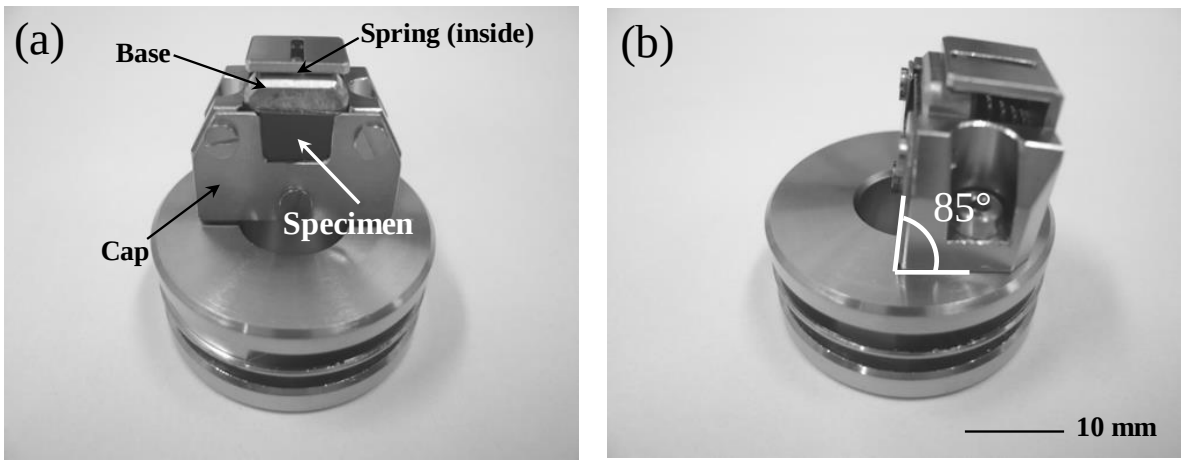

Fig. 1. Overview of the 85° high-angle inclined specimen holder.
(a) Front view and (b) Side view. (*J. Surf. Anal.* **24**, 192-205(2018)).

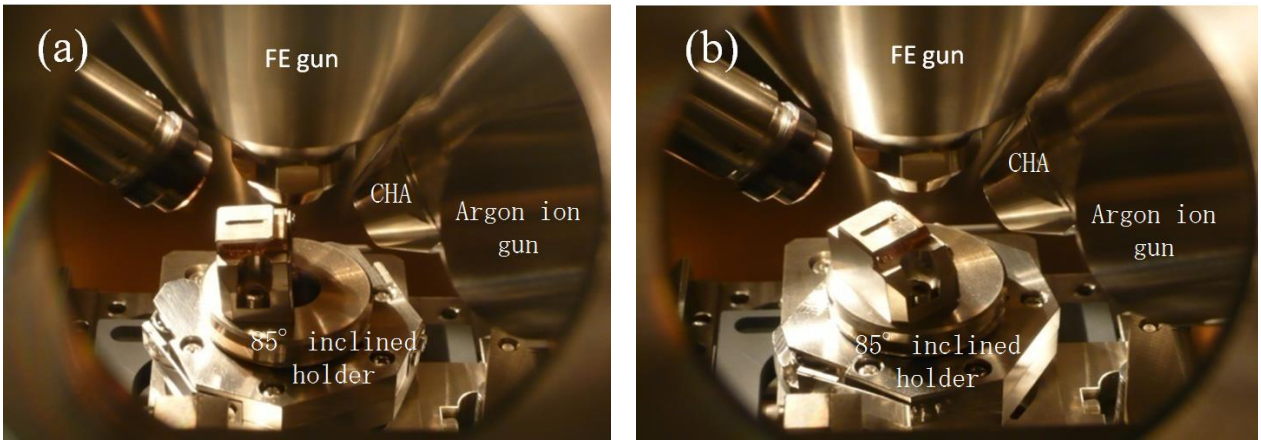

Fig. 2. Photographs of the 85° inclined specimen holder set on the stage at different azimuthal angles.
(a) The holder faces to the CHA side and (b) The holder is rotated by 35° from the CHA side. (*J. Surf. Anal.* **24**, 192-205(2018)).

Figs. 3(a), and (b) are TEM images of the 6 nm HfO_2 thin film on the Si substrate. A 2 nm amorphous layer with contrast different from that of HfO_2 was observed at the interface between the HfO_2 thin film and the Si substrate. Figs.4(a) - (d) were Si 2p spectra obtained by angle-resolved XPS, where the photoelectron take-off angles with respect to the surface normal were (a) 27.5°, (b) 42.5°, (c) 57.5°, and (d) 72.5°. The estimated Si 2p binding energy was 103 eV, which was suggested to be derived from SiO_2 native oxide and $HfSi_xO_y$ [10]. The Si 2p peak intensity from $HfSi_xO_y$ increased with increasing take-off angle, indicating that the layer-closer to the surface was $HfSi_xO_y$. Those results showed that the structure of the sample examined would be 55 nm HfO_2/2 nm ($HfSi_xO_y$+SiO_2)/Si.

2.3 Measurement conditions

Ultra-low-angle-incident ion beam Auger depth profiling was performed with the sample in an 85° high-inclination holder and an incident ion angle of 7° to the sample surface, as described above. Measurements were also performed with the usual flat sample holder inclined at 45° to the spectrometer side. These measurements were acquired with a JEOL JAMP-9500F scanning Auger microprobe equipped with a CHA electron spectrometer. Detailed measurement conditions

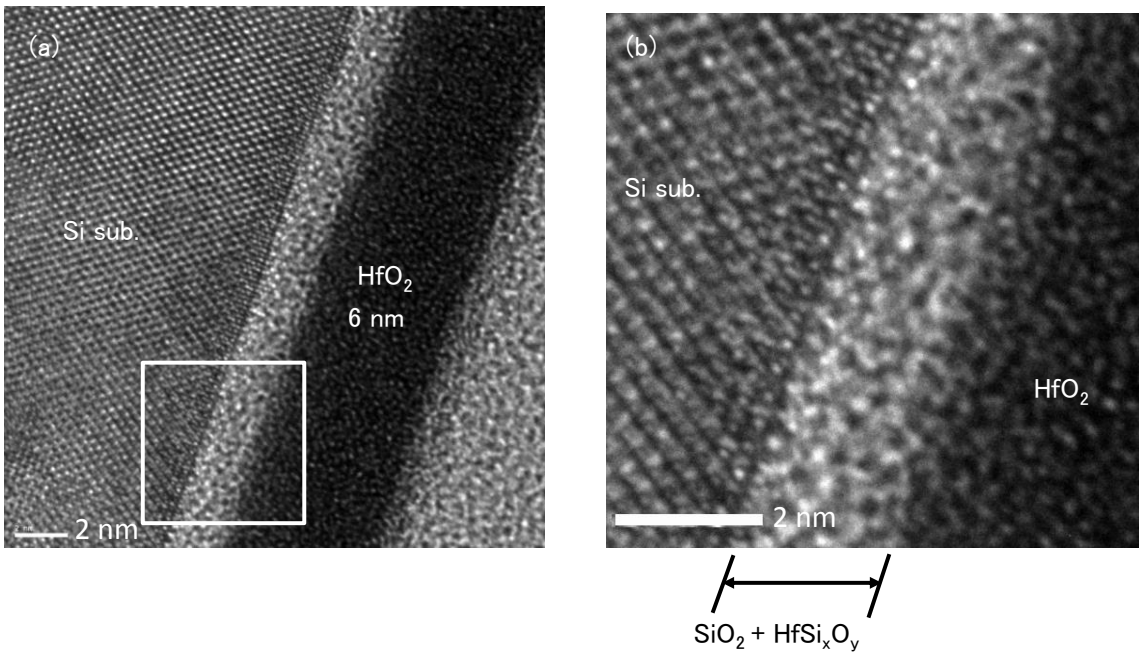

Fig. 3. TEM images of the interface between HfO_2:6nm thin film and Si substrate.
(a) A region observed about 22 nm square and (b) Enlarged □ region of (a). (*J. Surf. Anal.* **24**, 192-205(2018)).

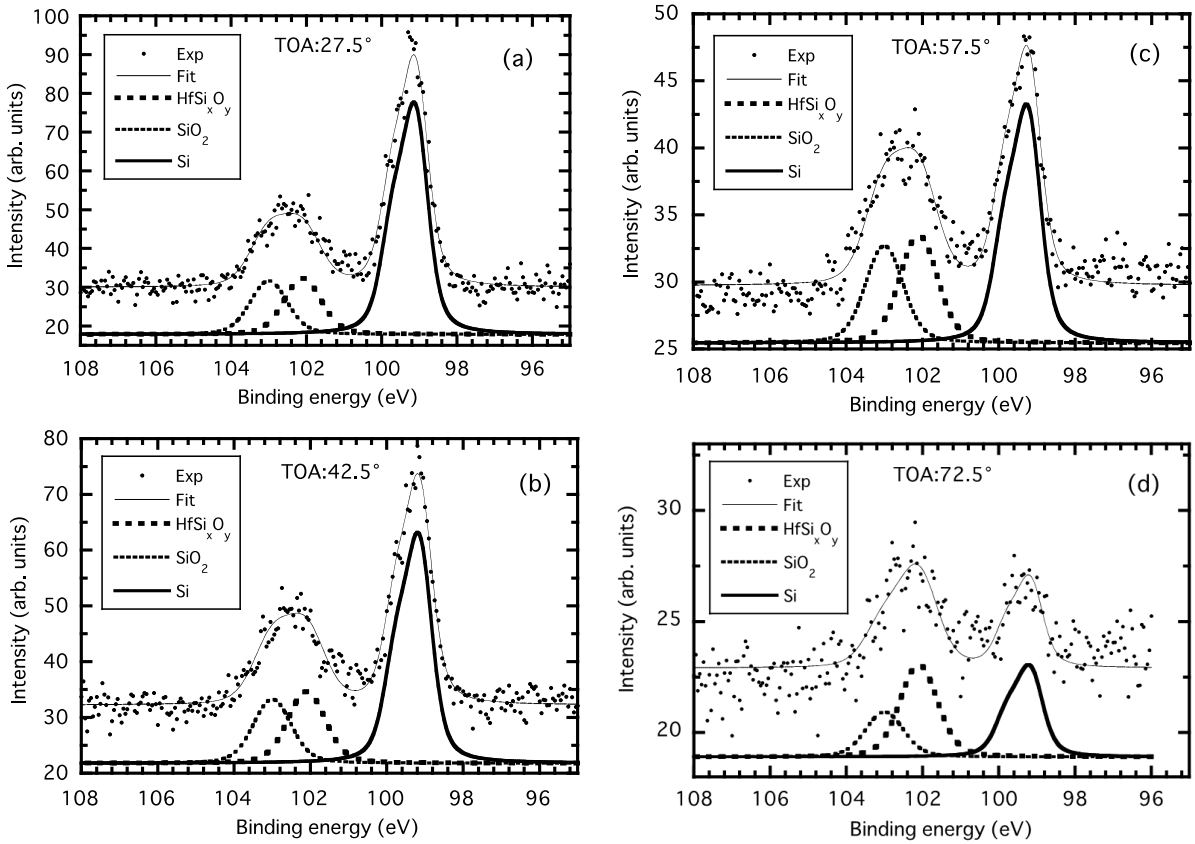

Fig. 4. AR-XPS spectra of Si 2p of surface of the HfO_2 : 3 nm thin film/Si substrate.
Take-off angle is (a) 27.5°, (b) 42.5°, (c) 57.5°, and (d) 72.5°. (*J. Surf. Anal*. **24**, 192-205(2018)).

were as follows.

2.3.1 Ultra-low-angle-incident beam method

Ar^+ ions sputtering was performed at the voltages of 0.5, 2.0, and 3.0 kV, and an 7° incident angle to the sample surface. The Auger peaks were measured with the primary electron beam at a 10 kV acceleration voltage, a 10 nA beam current, and an 5° incident angle to the sample surface. The electron beam diameter was 20 μm to reduce irradiation damage. The measured Auger peaks were Hf NVV (167 eV), O KLL (505 eV), Hf MNN (1624 eV), and Si KLL (1619 eV). The N(E) spectrum was measured for each Auger peak under a constant analyzing energy mode (100 eV pass energy). The depth profile was obtained from each differential spectrum. Differential spectra were obtained by numerical differentiation (seven points) of the N(E) spectrum. The differences between the maximum and the minimum intensities of the differential spectrum were plotted against the sputtering time to obtain the depth profile. Overlapping peaks between Hf MNN (1624 eV) and Si KLL (1619 eV) were separated by a nonlinear least squares method [11]. The sputtering time at the midpoint was read from the interface depth profile of oxygen obtained with the ion accelerating voltage of 0.5, 2.0, 3.0 kV, and the sputtering rate was obtained by dividing the film thickness of HfO_2 by 55 nm at those times. Using these sputtering rates, the X-axis sputtering time of the profile was converted to thickness.

The depth resolution was defined as the distance between 84% and 16% of the intensity change at an interface.

2.3.2 Conventional method

Ar^+ ions was accelerated at acceleration voltages of 0.5, 1.0, 2.0, and 3.0 kV, and the incident angle was 51°to the sample surface. The primary electron beam incident angle was 45° to the sample surface. All other measurement conditions and procedures were the same as those described in Sec.2.3.1.

3. Results and discussion

3.1 Depth profiles obtained by ultra-low-angle-incident beams

Auger depth profiles measured at ion acceleration voltages of 0.5 kV, 2.0 kV, and 3.0 kV with ultra-low-angle-incident beams were plotted in Figs. 5 - 8. Because the 0.5 kV ion sputtering rate in Fig.5 was very low, it was difficult to measure the depth profile down to the Si substrate. Therefore, this measurement was terminated at a sputtering time of 300 min, before reaching the Si. The measurements at the 2.0 kV ion acceleration voltage were repeated twice for repeatability. The results are shown in Figs. 6, 7.

As shown in Figs. 6 - 8, the intensity of the O KLL depth profile decreases by 20 - 30% until the depth of 5 nm from the start of the measurement. In Fig.5, the intensity of the O KLL depth profile acquired with 0.5 kV ions was halved after 250 min sputter time.

Using the depth profiles of O KLL and Hf NVV in Figs. 6 - 8, the average intensity was obtained from the

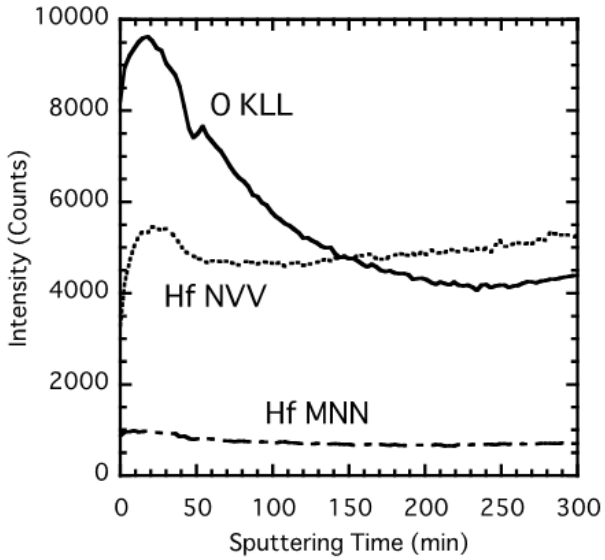

Fig. 5. AES depth profile of the HfO_2:55 nm/Si substrate using the ultra low angle incident beam method with the argon ion energy of 0.5 keV. (*J. Surf. Anal.* **24**, 192-205(2018)).

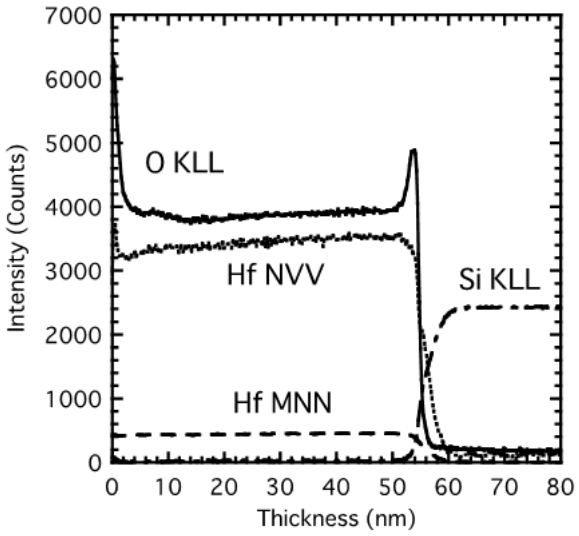

Fig. 6. 1st AES depth profile of the HfO_2:55 nm/Si substrate using the ultra low angle incident beam method with the argon ion energy of 2.0 keV. (*J. Surf. Anal.* **24**, 192-205(2018)).

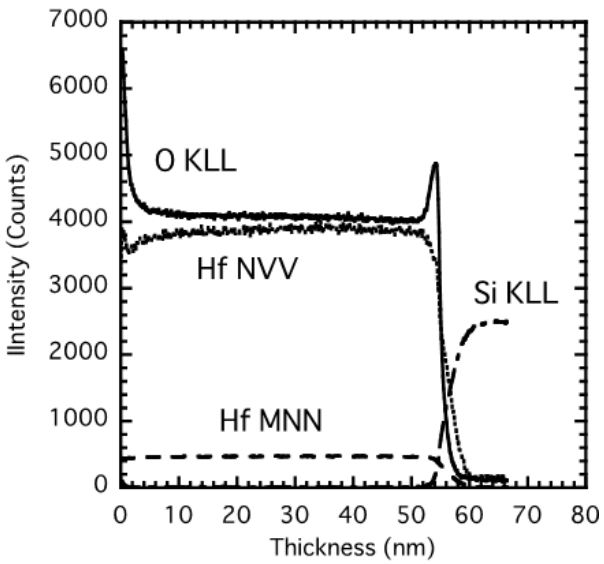

Fig. 7. 2nd AES depth profile of the HfO_2:55 nm/Si substrate using the ultra low angle incident beam method with the argon ion energy of 2.0 keV. (*J. Surf. Anal.* **24**, 192-205(2018)).

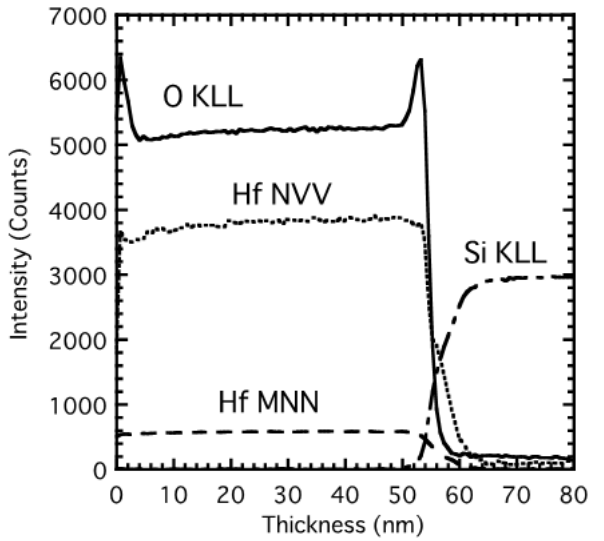

Fig. 8. AES depth profile of the HfO_2:55 nm/Si substrate using the ultra low angle incident beam method with the argon ion energy of 3.0 keV. (*J. Surf. Anal.* **24**, 192-205(2018)).

intensity of 10 to 40 nm in depth. From the average intensity, the intensity ratio of O KLL and Hf NVV was determined and compared. The O KLL and Hf NVV depth profiles in Figs. 6 - 8 indicated that their intensity ratios for 2.0 kV ions were 1.15 and 1.05 in Fig.6 and Fig.7, respectively. That for 3.0 kV ions in Fig.8 was 1.37. For the 0.5 kV ions in Fig.5, the O KLL and Hf NVV intensities were reversed at the depth corresponding to a 150 min sputtering time. Thus, when sputtering was performed at a 7°incidence angle, the Hf and O sputtering yields in the HfO_2 film depended on the ion acceleration voltage. At lower voltages, the O sputter yield was higher than that of Hf.

As shown in Figs. 6 - 8, the intensity of the O KLL depth profiles near the HfO_2/Si interface sharply increased by 20%. Then, it exhibited the similar intensity reduction as the Hf NVV profile to the depth of 55 nm, even at the depth after that, the strength suddenly decreased, which was a sharp interface profile. On the other hand, the profile of Hf NVV overlapped with the profile of the Si substrate considerably under the depth of about 55 nm.

Table 1 lists the depth resolutions derived from the O KLL depth profiles in Figs. 6 - 8. The values obtained

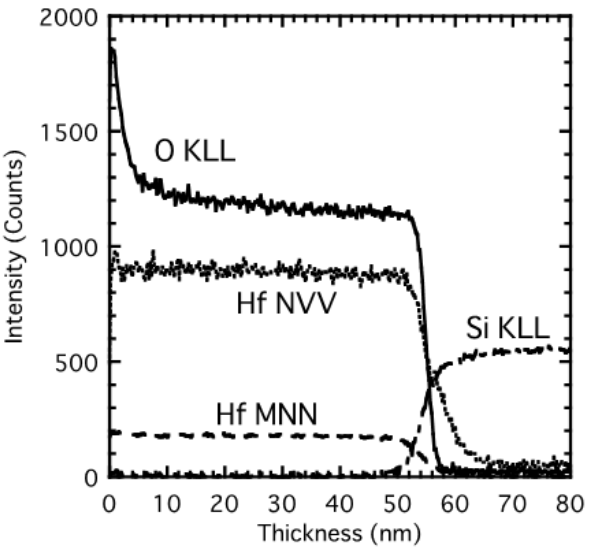

Fig. 9. AES depth profile of the HfO_2:55 nm/Si substrate using the conventional method with the argon ion energy of 0.5 keV. (*J. Surf. Anal.* **24**, 192-205(2018)).

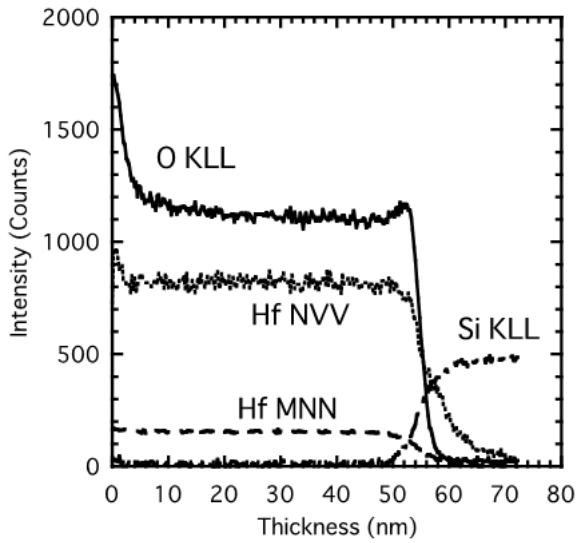

Fig. 10. AES depth profile of the HfO_2:55 nm/Si substrate using the conentional method with the argon ion energy of 1.0 keV. (*J. Surf. Anal.* **24**, 192-205 (2018)).

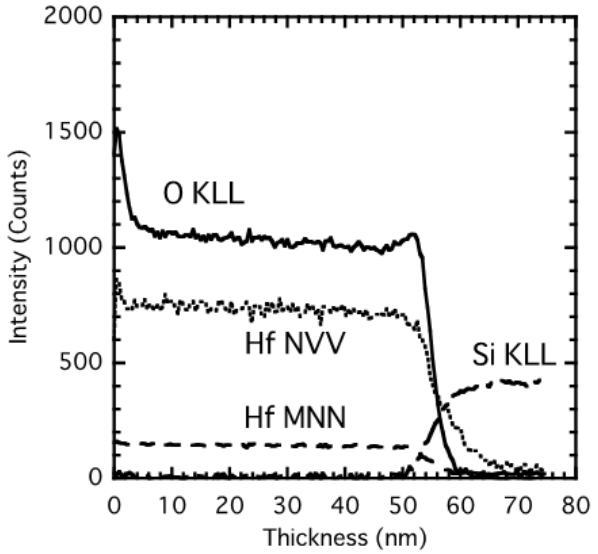

Fig. 11. AES depth profile of the HfO_2:55 nm/Si substrate using the conventional method with the argon ion energy of 2.0 keV. (*J. Surf. Anal.* **24**, 192-205(2018)).

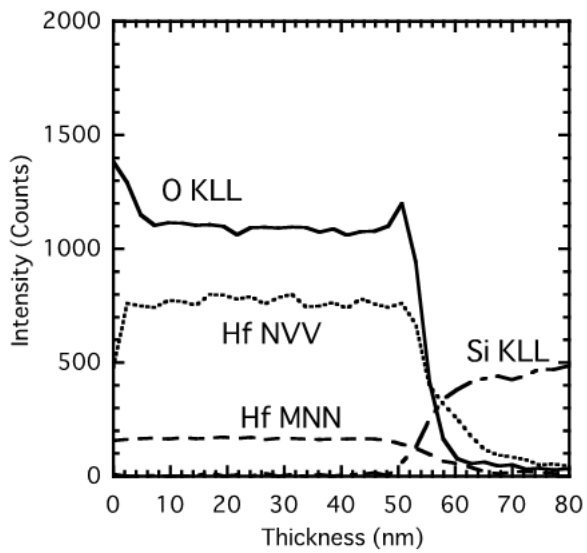

Fig. 12. AES depth profile of the HfO_2:55 nm/Si substrate using the conventional method with the argon ion energy of 3.0 keV. (*J. Surf. Anal.* **24**, 192-205 (2018)).

Table 1. Depth resolution of the O KLL interface profiles (*J. Surf. Anal*. **24**, 192-205(2018)).

Method	Ion energy（kV）	Depth resolution（nm）
Conventional method	0.5	2.2
	1.0	2.7
	2.0	3.5
	3.0	4.6
Ultra low angle incident beam method	2.0（Fig.6）	0.9
	2.0（Fig.7）	1.5
	3.0	1.5

with the ultra-low-angle-incident beam method were 0.9 - 1.5 nm, which were about 1/3 those measured with the conventional method at the same ion acceleration voltages.

3.2 Depth profiles obtained with the conventional method

The Auger depth profiles measured with the conventional method at ion acceleration voltages of 0.5 - 3.0 kV were plotted in Figs. 9 - 12. The intensities of the O KLL depth profile decreased by 20 - 30% at the depth of 5 nm from the surface.

The intensity ratios of O KLL and Hf NVV were obtained from the depth profiles in Figs. 9 - 12. They were 1.3, 1.4, 1.4, and 1.5, for ion acceleration voltages of 0.5, 1.0, 2.0, and 3.0 kV, respectively. The results showed that the Hf and O yields in the HfO_2 film did not depend significantly on the ion acceleration voltage, when the sputtering was performed at an ion incidence angle of 51°in the conventional method.

As shown in Figs. 10 - 12, the O KLL depth profiles at the HfO_2/Si interface exhibited a characteristic shape that slightly increased in intensity. In Fig.9, the O KLL depth profile at the 0.5 kV voltage showed no increase in intensity at the interface. The difference of depth profiles at the interface will be discussed in Sec. 3.5. In addition, the Hf NVV profile near the interface substantially enters the Si substrate below a depth of 55 nm. At higher ion acceleration voltages, the Hf NVV profiles entered deeper into the Si substrate.

Table 1 listed the depth resolution values derived from the O KLL depth profiles in Figs. 9 - 12. The depth resolution was better at lower ion acceleration voltages; it was 2.2 nm at the lowest voltage of 0.5 kV examined.

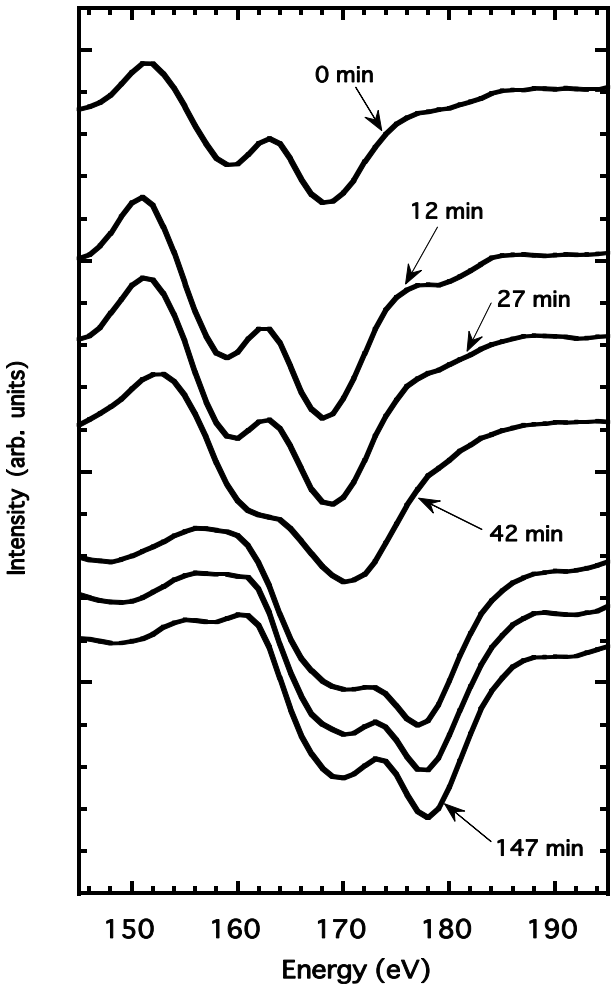

Fig. 13. Raw data of the Hf NVV depth profile of the HfO_2:55 nm/Si substrate using the ultra low angle incident beam method with the argon ion energy of 0.5 keV. (*J. Surf. Anal.* **24**, 192-205 (2018)).

3.3 Reduction of HfO_2 by Argon Ion Irradiation

When HfO_2 was irradiated with argon ions, preferential sputtering of oxygen occurred and it was reduced to HfO_x [12]. We investigated the Hf NVV spectrum was examined to elucidate whether reduction of HfO_2 could be suppressed when measured at the 0.5 kV ion voltage and a low incident angle. This was shown in Fig. 13.

The Hf NVV spectrum in Fig. 13 was from the surface (0 min sputtering) to 147 min sputtering. The spectrum at 0 min had peaks at 168 eV and 158 eV. The spectrum after sputtering for 12 min had similar profile to that at 0 min, with similar peak intensities. After 27 min of sputtering, the peak shifted to 169 eV and 159 eV, and to 170 eV after 42 min of sputtering. After further sputtering, peaks at 178 eV and 170 eV were observed. Thus, ion-beam-induced reduction of HfO_2 had occurred

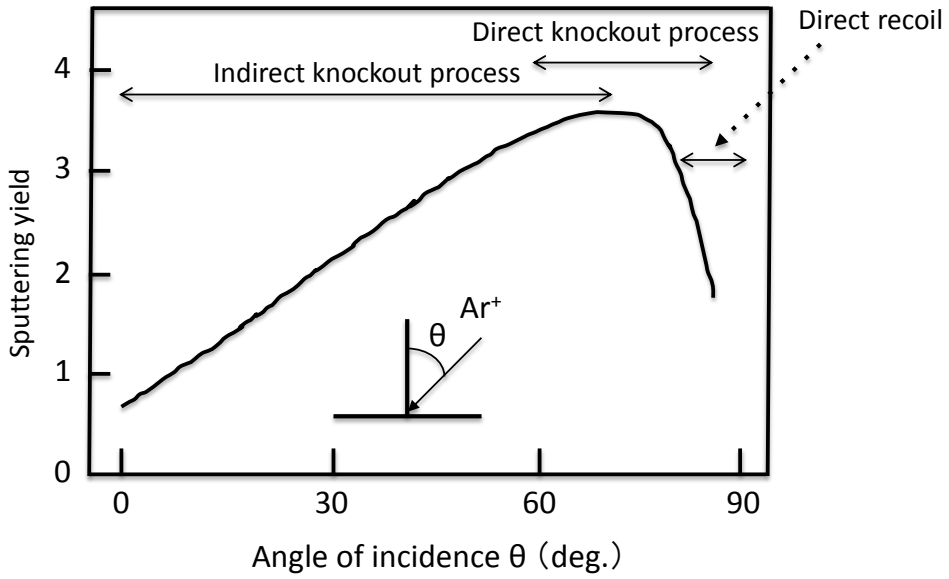

Fig. 14. Schematic diagram of angular dependence of sputtering yield with an incident light ion. (*J. Surf. Anal.* **24**, 192-205 (2018)).

and was not suppressed by the low damage of a glancing-angle ion beam at 0.5 kV.

3.4 Intensity ratios of O KLL and Hf NVV in depth profiles

As discussed in Sec. 3.1 and Sec. 3.2, the O KLL and Hf NVV intensity ratios in the depth profiles were almost independent of the ion acceleration voltage in the conventional method. Whereas, in the ultra- low- angle-incident beam method they depended on the voltage, and O was more easily sputtered than Hf. These are discussed from the relationship between sputtering yield of target atoms, ion incidence angle, ion acceleration voltage as follows.

Fig. 14 is a schematic diagram showing the relationship between ion incidence angle and sputter yield for light ions. In the collision cascade model of sputtering, incident ions repeatedly collide with target atoms, and the target atoms in turn form a collision cascade that changes atomic positions. Sputtering occurs when the cascade reaches the surface. However, when light ions are incident on heavy target atoms, the ions mainly move in the sample and a collision cascade does not form. In this case, sputtering occurs when the light ions inside the sample move back toward the surface and collide with heavy surface atoms in a knockout process proposed by Yamamura et al. [13-15]. There are “direct” and “indirect” knockout processes. When the ion incident angle measured from the direction perpendicular to the surface is large, direct knockout is primary. However, as the incident angle decreases, indirect knockout becomes primary. Direct knockout is the sputtering where direct kinetic energy transfer occurred from a primary recoil atom to the target atom; i.e., in the process, directly sputtered by elastic collision of the ions and target atoms. Indirect knockout occurs when light ions are backscattered by colliding with target atoms, and pass back throughout the surface.

As shown in Fig.14, the yield increased with the increment in ion incident angle θ, and the sputtering yield reached the maximum value at angles of 60 - 80 degrees. In addition, as the ion incidence angle increased, the incident ions were almost reflected without transferring the energy to the surface target atoms. Hence, sputtering (direct recoil) did not occur, and the sputtering yield sharply decreased [16]. When the ion acceleration voltage decreased, the incidence angle where the sputtering yield was the maximum, decreased [17-18]. Furthermore, when the mass of the target atom was larger than ion mass, the sputtering yield decreased [19].

The 7° of the ion incident angle in the present study, corresponded to the angle at which the sputtering yield reached the maximum or decreased steeply, proposed by Yamamura et al.. The critical ion incidence angle for the maximum sputtering yield decreased at lower ion acceleration voltages. At extremely low incident angles

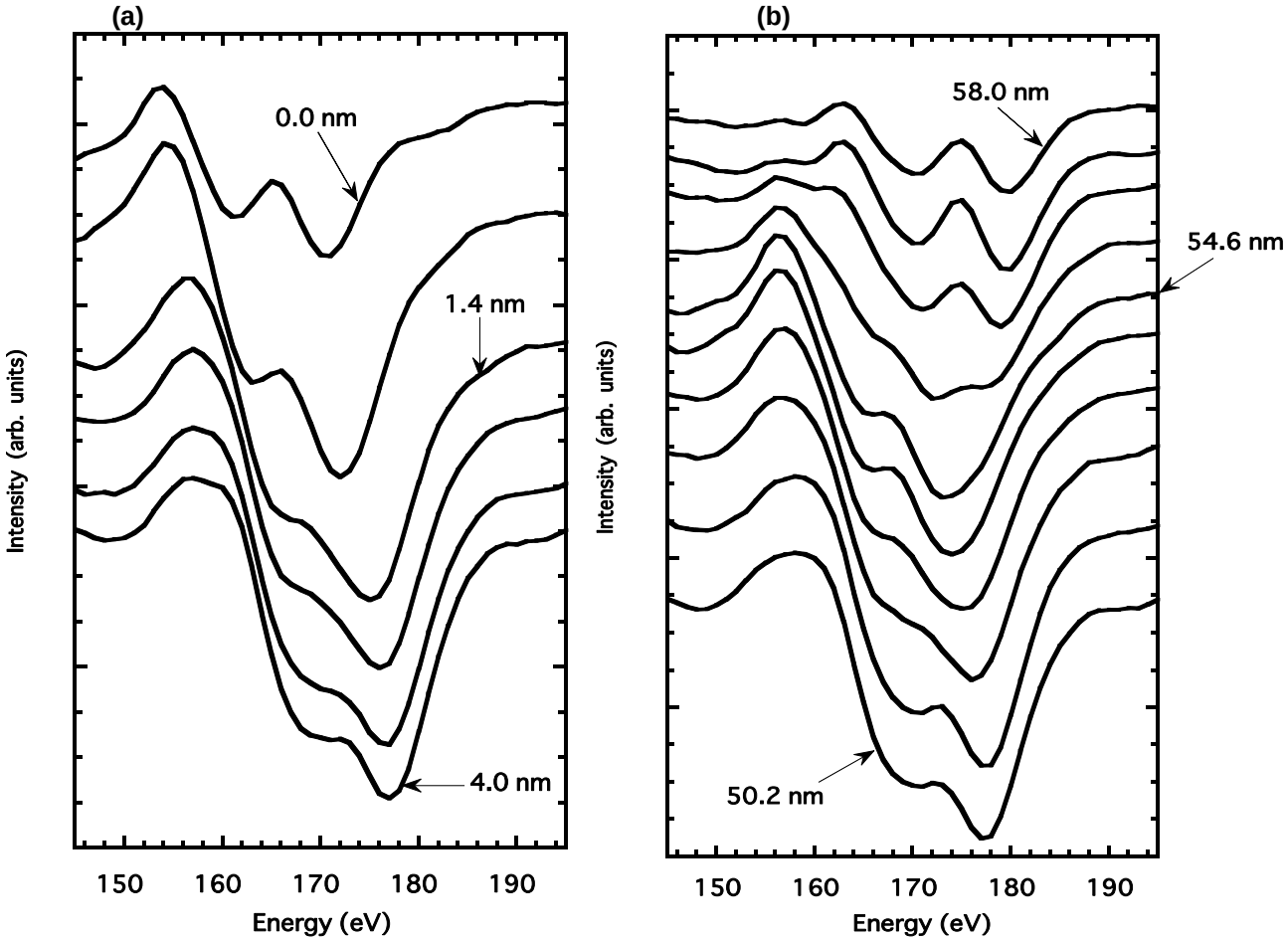

Fig. 15. (a)Raw data near the surface of the Hf NVV depth profile of the HfO_2:55 nm/Si substrate using the ultra low angle incident beam method with the argon ion energy of 3.0 keV. (b) Raw data near the interface of the Hf NVV depth profile of the HfO_2:55 nm/Si substrate using the ultra low angle incident beam method with the argon ion energy of 3.0 keV. (*J. Surf. Anal.* **24**, 192-205 (2018)).

and low ion acceleration voltages, the sputtering yield would greatly decrease. The critical angle depended not only on the voltage but also on the ion/target mass ratios. The incident Ar^+ (39.9) to Hf (178.5) and O (16.0) target ratios were 4.5 and 0.4, respectively. Thus, when HfO_2 was irradiated with Ar^+, O atoms were more likely to be sputtered, and the intensity ratios of the O KLL and Hf NVV depth profiles depended on the ion acceleration voltages at the low incident angles. The depth profiles in Figs. 6, and 7 were measured under the same conditions at an ion voltage of 2.0 kV. The difference in the intensity ratios of the O KLL and Hf NVV depth profiles may have been caused by a slight deviation in the position adjustment of the sample holder affecting the ion incident angle, because; the sputtering yield was influenced by very sensitively to the incident angles, especially to the ultra-low-incidence angles. Therefore, it is important to confirm reproducibility of the data, when irradiating heavy targets with an ultra-low-angle incident beam.

In contrast, at the 51° incidence angle of the conventional method, indirect knockout occurs. In this case, the sputtering yield dependence on ion acceleration voltage was not significant, being roughly linear. Thus, the O KLL and Hf NVV intensity ratios in the depth profiles did not depend much on ion acceleration voltage.

3.5 Increase in O KLL depth profile intensity at the interface

Hf NVV spectra from the surface (0.0 nm) to a depth of 4.0 nm, obtained for the Hf NVV depth profiling (Fig. 8), were superimposed in Fig. 15(a). The spectrum at the surface had peaks at 170 eV and 161 eV. Depending on the sputtering depth, the peak positions shifted to higher kinetic energies, and the two peaks coalesced. The peak

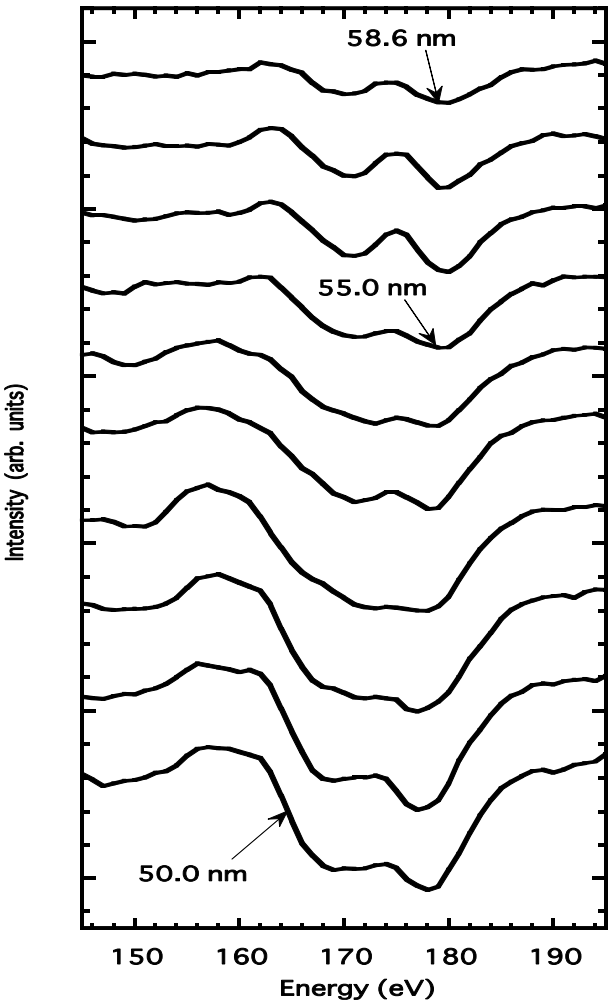

Fig. 16. Raw data near the interface of the Hf NVV depth profile of the HfO_2:55 nm/Si substrate using the conventional method with the argon ion energy of 0.5 keV. (*J. Surf. Anal.* **24**, 192-205 (2018)).

at 177 eV was detected at the 4.0 nm depth.

Hf NVV spectra near the interface at depths of 50.2 - 58.0 nm, obtained for the Hf NVV depth profiling (Fig. 8), were superimposed in Fig. 15(b). These spectra were measured at positions where the O KLL depth profile intensity abruptly increased at the interface. In Fig. 15(b), the Hf NVV spectrum at a depth of 50.2 nm had a peak at 177 eV and a shoulder at 170 eV, which were the same as those at a depth of 4.0 nm in Fig. 15(a). The Hf NVV peak positions shifted to lower kinetic energy from a depth of 50.2 nm to 54.6 nm. The spectrum at 54.6 nm had a peak at 173 eV. The peaks in the spectra at the positions deeper than 54.6 nm shifted back to higher kinetic energies. At the depth of 58.0 nm, peaks were detected at 180 eV and 170 eV.

In Fig.16 is plotted the Hf NVV spectrum at the

Table 2. Penetration depth of Hf into Si substrate obtained from Hf NVV profiles (*J. Surf. Anal*. **24**, 192-205(2018)).

Method	Ion energy (kV)	Penetration depth (nm)
Conventional method	0.5	10
	1.0	14
	2.0	20
	3.0	25
Ultra low angle incident beam method	2.0	4
	2.0	5
	3.0	5

interface from depths of 50 - 58.6 nm, at an ion acceleration voltage of 0.5 kV with the conventional method. The Hf NVV spectrum at 50.0 nm had peaks at 178 eV and 168 eV. At deeper depths, the peak positions shifted to higher kinetic energies; at a depth of 58.6 nm, the peaks were detected at 180 eV and 170 eV. Those spectra at the 0.5 kV showed that the peak position shifted only to higher kinetic energies, without the peak shifts to the lower kinetic energies, at 3.0 kV in Fig. 15(b).

These results suggested as follows: the chemical reduction occurred near the sputtered HfO_2 surface, and the Hf NVV peaks shifted from 170 eV to 177 eV. During the depth profiling, the reduced state was maintained from a depth of 4.0 nm to the interface. However, the Hf NVV peak shifts in Fig. 15(b) suggested that, the reduced HfO_x took in oxygen at the interface and was re-oxidized to HfO_2. The re-oxidization would explain that the O KLL peak intensities rose sharply.

The re-oxidation would depend on the oxygen supplied by SiO_2 and $HfSi_xO_y$ in a 2 nm thick amorphous layer at the HfO_2/Si interface (described in Sec. 2.2). This layer would be a diffusion layer where the SiO_2 and $HfSi_xO_y$ composition gradually changed [20]. When the diffusion layer was irradiated, it decomposed and oxygen was supplied to HfO_x. Figure 16 indicated that the layer did not decompose by the sputtering at 0.5 kV, which means that an oxygen supply to HfO_x did not occur. This was consistent with the result shown in Fig. 9, where no increase in signal intensities of the O KLL depth profile was observed at the interface. In addition, the peak shift to the lower kinetic energy was not observed in the Hf NVV spectrum in Fig. 16, and the oxygen supply to

HfO_x was not expected to occur at an ion acceleration voltage of 0.5 kV.

3.6 Penetration of the Hf NVV at the interface into the Si substrate

As described in Sec. 3.1 and Sec. 3.2, the Hf profile suggested that Hf NVV might penetrate into the Si substrate of the interface with either methods. Table 2 lists the penetration depth (nm) as calculated from the spectra shown in Figs. 6 - 8 and Figs. 9 - 12. In the conventional method, the penetration depth depended on the ion acceleration voltage. At 3.0 kV, the penetration depth was 25 nm. In contrast, the penetration depth for the 3.0 kV data was 5 nm for the ultra-low-angle-incident beam. This was half of the penetration depth at the lowest ion acceleration voltage of 0.5 kV for the conventional method.

Generally, recoil implantation occurs when film atoms are injected into the substrate, when a thin film sample is irradiated with an ion beam. Film elements heavier than those of the substrate are more effectively recoil-implanted [21]. In the present study, the sample is a thin film containing heavy element Hf (178.5) on the Si (28.1) substrate. Therefore, the heavier element Hf (178.5) penetrated deep into the Si (28.1) substrate during the depth profiling for the conventional method, because of recoil implantation of Hf into the Si and formation of silicide[22]. While, by the ultra-low-angle-incident beam, the penetration depth of Hf at 3.0 kV was 5 nm, and recoil implantation was not detected. The thickness of the interface layer ($HfSi_xO_y$+SiO_2) shown in the TEM image of Fig. 3 is 2 nm and the depth resolution of O KLL is 1.5 nm, the thickness of the silicide is estimated to be about 4 nm. Therefore, the penetration depth of Hf in the Si substrate for the low angle beam (Table 2) will accurately reflected the thickness of the Hf silicide.

4. Conclusions

Auger depth profiles of HfO_2/Si was investigated with an ultra-low-angle-incident beam and conventional methods. The following was observed:

(1) The depth resolution of the HfO_2/Si interface depended on the ion acceleration voltage. Better depth resolution was obtained at lower voltages. It was 0.9 - 1.5 nm with the low angle method, which was about 1/3 that with the conventional method.

(2) The low angle method at a 0.5 kV ion acceleration voltage produced the least damage to the sample surface, although, it was still found that reduction of HfO_2 by sputtering occurred.

(3) At an ion incidence angle of 7 ° for the low angle method, the intensity ratios of the O KLL and Hf NVV depth profiles greatly depended on the ion acceleration voltage. At low voltages, O was more likely to be sputtered than Hf.

(4) The O KLL depth profile with the low angle method had a characteristic shape near the surface and the interface. This was related to reduction of the surface by ion sputtering and re-oxidation of the reduction layer in the interface region.

(5) The ultra-low-angle-incident beam method exhibited very little recoil implantation.

5. References

[1] T. Ogiwara, T. Nagatomi, K. J. Kim, and S. Tanuma, Hyoumen Kagaku **32**, 664 (2011).

[2] National Institute of Advanced Industrial Science and Technology, NIMC CRM 5201-a, GaAs/AlAs Superlattice Reference Material.

[3] National Institute of Advanced Industrial Science and Technology, NMIJ CRM 5202-a, SiO_2/Si Multilayer Film.

[4] T. Ogiwara, T. Nagatomi, K. J. Kim, and S. Tanuma, *J. Surf. Anal.* **18**, 174 (2012).

[5] S. Sugimoto, T. Kamigaki and H. Kamijo , *TOSHIBA review* **59**, 2 (2004).

[6] M. Haemori, T. Nagata, and T. Chikyow, *Applied Physics Express* **2**, 061401 (2009).

[7] J. Müller, T. S. Böscke, D. Bräuhaus, U. Schröder, U. Böttger, J. Sundqvist, P. Kücher, T. Mikolajick, and L. Frey, *Appl. Phys. Lett.* **99**, 112901 (2011).

[8] ISO18115-1 - *Surface Chemical Analysis* – Vocabulary - Part 1 : General terms and terms used in spectroscopy, International Organization for Standardization, Geneva (2010).

[9] Pulsed Laser Deposition of Thin Films, ed. by R. Eason, John Wiley & Sons, 2007.

[10] Y. Oniki, Y. Iwazaki, M. Hasumi, T. Ueno, and K. Kuroiwa, *Jpn. J. Appl. Phys.* **48**, 05DA01 (2009).

[11] N. Ikeo, *JEOL Application Note*, AP78 (1995).

[12] J. M. Sanz, *Vacuum*, **37**, 445 (1987).

[13] Y. Yamamura, T. Takiguchi and Z. Li , *Kakuyugokenkyuu* **66**, 277 (1991).
[14] T. Ono, T. Kenmotsu, and T. Muramoto, Simulation of the Sputtering Process in Reactive Sputter Deposition, edited by D. Depla and S. Mahieu, SPRINGER SERIES IN MATERIALS SCIENCE 109 (2008).
[15] T. Kenmotsu, Ph. D. thesis, Okayama University of Science, 1998）
[16] Y. Yamamura, Hyoumen Kagaku **11**, 581 (1990).
[17] T. Ono, M. Ono, K. Shibata, T. Kenmotsu, Z. Li, T. Kawamura, National Institute for Fusion Science (NIFS) report number NIFS-DATA-114 (2012).
[18] A. Oliva-Florio, R. A. Baragiola, M. M. Jakas, E. V. Alonso and J. Ferron, *Phys. Rev. B* **35**, 2198 (1987).
[19] R. V. Stuart, Vacuum Technology, Thin Films, and Sputtering An Introduction, Academic Press, (1983).
[20] M. Quevedo-Lopez, M. El-Bouanani, S. Addepalli, J. L. Duggan, B. E. Gnade, R. M. Wallace, M. R. Visokay, M. Douglas, and L. Colombo, *Appl. Phys. Lett.,* **79**, 4192 (2001).
[21] R. A. Moline, RECOIL IMPLANTATION in Ion Implantation in Semiconductors 1976, edited by Fred Chernow, James A. Borders and David K. Brice (Springer,1977).
[22] S. Zaima and Y. Yasuda, *OYOBUTURI* **63**, 1093 (1994).